Research in Astron. Astrophys. **2010** Vol. **10** No. **11**, 1109–1118
http://www.raa-journal.org *http://www.iop.org/journals/raa*

Research in Astronomy and Astrophysics

Cosmological constraints on the Undulant Universe *

Tian Lan[1,2], Yan Gong[2,3], Hao-Yi Wan[4] and Tong-Jie Zhang[1,5]

[1] Department of Astronomy, Beijing Normal University, Beijing 100875, China
[2] National Astronomical Observatories, Chinese Academy of Sciences, Beijing 100012, China
[3] Graduate University of Chinese Academy of Sciences, Beijing 100049, China
[4] Business Office, Beijing Planetarium, Beijing 100044, China
[5] Center for High Energy Physics, Peking University, Beijing 100871, China; *tjzhang@bnu.edu.cn*

Received 2010 March 1; accepted 2010 June 15

Abstract We use the redshift Hubble parameter $H(z)$ data derived from relative galaxy ages, distant type Ia supernovae (SNe Ia), the Baryonic Acoustic Oscillation (BAO) peak, and the Cosmic Microwave Background (CMB) shift parameter data, to constrain cosmological parameters in the Undulant Universe. We marginalize the likelihood functions over h by integrating the probability density $P \propto e^{-\chi^2/2}$. By using a Markov Chain Monte Carlo (MCMC) technique, we obtain the best fitting results and give the confidence regions in the $b - \Omega_{\rm m0}$ plane. Then we compare their constraints. Our results show that the $H(z)$ data play a similar role with the SNe Ia data in cosmological study. By presenting the independent and joint constraints, we find that the BAO and CMB data play very important roles in breaking the degeneracy compared with the $H(z)$ and SNe Ia data alone. Combined with the BAO or CMB data, one can remarkably improve the constraints. The SNe Ia data sets constrain $\Omega_{\rm m0}$ much tighter than the $H(z)$ data sets, but the $H(z)$ data sets constrain b much tighter than the SNe Ia data sets. All these results show that the Undulant Universe approaches the ΛCDM model. We expect more $H(z)$ data to constrain cosmological parameters in the future.

Key words: cosmology: observations — dark matter

1 INTRODUCTION

Many cosmological observations (Bennett et al. 2003; Spergel et al. 2007; Eisenstein et al. 2005; Kowalski et al. 2008), such as distant SNe Ia (Riess et al. 1998; Perlmutter et al. 1999), the subsequent Cosmic Microwave Background (CMB measurement by the Wilkinson Microwave Anisotropy Probe (WMAP) (Spergel et al. 2003) and the large scale structure survey by the Sloan Digital Sky Survey (SDSS) (Tegmark et al. 2004a; Tegmark et al. 2004b), etc., support that our Universe is undergoing an accelerated expansion, and these data have mapped the universe successfully by constraining cosmological parameters (Perlmutter et al. 1999; Tegmark et al. 2000; Zhu 2004; Zhan et al. 2006; Lineweaver 1998; Efstathiou 1999; Zhan et al. 2005; Maartens et al. 2006). Meanwhile, many different observations, such as the related redshift-dependent quantities, are usually used. The luminosity distance to a particular class of objects, e.g. SNe Ia and Gamma-Ray Bursts (GRBs)

* Supported by the National Natural Science Foundation of China.

(Nesseris & Perivolaropoulos 2004), the size of the Baryonic Acoustic Oscillation (BAO) peak detected in the large-scale correlation function of luminous red galaxies from SDSS (Eisenstein et al. 2005) and the CMB data obtained from the three-year WMAP estimate (Wang & Mukherjee 2006; Spergel et al. 2007) are redshift-dependent. The BAO and CMB data have been combined to widely constrain the cosmological parameters. Recently, the Hubble expansion rate at different redshifts can be directly obtained from the measurement of relative galaxy ages. As a function of redshift z, the $H(z)$ data have been used to test cosmological models (Gong et al. 2008; Yi & Zhang 2007; Samushia & Ratra 2006; Wei & Zhang 2007a; Zhang et al. 2007; Wei & Zhang 2007b; Zhang & Wu 2007; Dantas et al. 2007; Zhang & Zhu 2007; Wu & Yu 2007; Wei & Zhang 2007a). Using different data to constrain parameters can provide the consistency checks between each other, and the combination of different data can also make the constraints tighter (Li et al. 2008; Zhao et al. 2007; Xia et al. 2006). So far, few works have been done to compare the respective results. We would like to study the comparison of the SNe Ia, $H(z)$, BAO and CMB data in this paper. Many cosmological models, e.g. the Quintessence (Caldwell et al. 1998), the brane world (Deffayet et al. 2002), the Chaplygin Gas (Alcaniz et al. 2003) and the holographic dark energy models (Ke & Li 2005), have been extensively explored to explain the observed acceleration of the universe. The ΛCDM model, which is a standard and popular model, has been studied by Lin et al. (2009). In fact, there are some problems in the standard model, and this model is not consistent with the real universe. Scientists have also proposed an Undulant Universe, which is characterized by alternating periods of acceleration and deceleration (Barenboim et al. 2005). This model can remove the fine tuning problem (Vilenkin 2001; Garriga et al. 1999; Bludman 2000; Garriga & Vilenkin 2001; Stewart 2000), and solve the coincidence scandal between the observed vacuum energy and the current matter density, with some details given in Peebles & Ratra (2003). The equation of state (EOS) of the Undulant Universe is

$$\omega(a) = -\cos(b\ln a), \tag{1}$$

where the dimensionless parameter b controls the frequency of the accelerating epochs. Since most inflation models predict $\Omega_k < 10^{-5}$ (Tegmark & Rees 1998), we assume spatial flatness, so the Hubble parameter is

$$H^2(a) = H_0^2\Big(\Omega_{\rm m0}a^{-3} + \Omega_{\Lambda 0}a^{-3}\exp\Big[\frac{3}{b}\sin(b\ln a)\Big]\Big), \tag{2}$$

where $\Omega_{\rm m0}$, $\Omega_{\Lambda 0}$ are the density parameter of matter and dark energy, respectively. Furthermore, Nesseris and Perivolaropoulos have elaborated on the fact that an oscillating expansion rate ansatz has provided the best fit to the data among many ansatzes by using recent supernova data (Nesseris & Perivolaropoulos 2004).

In this paper, we concentrate on the comparison of different data sets in the Undulant Universe. In Section 2, we simply introduce the data sets that we use. Then the constraints are shown in Section 3. Finally, we show some important conclusions and discussions in Section 4.

2 OBSERVATIONAL DATA

2.1 SNe Ia Data

There have been some calibrated SNe Ia data measured with high confidence in Kowalski et al. (2008). This data set contains 307 datapoints and the redshifts of these data span the range of about 0.01 to 1.75. These data give luminosity distances $d_{\rm L}(z_i)$ and the redshifts z_i of the corresponding SNe Ia. In a Friedmann-Robertson-Walker (FRW) cosmology, considering a flat universe, the luminosity distance is

$$d_{\rm L}(z) = \frac{c(1+z)}{H_0}\mathcal{F}(z). \tag{3}$$

The function $\mathcal{F}(z)$ is defined as $\mathcal{F}(z) = \int_0^z \mathrm{d}z/E(z)$, with

$$E(z) = H(z)/H_0 = \sqrt{\Omega_{M0}a^{-3} + \Omega_{\Lambda 0}a^{-3}\exp\left[\frac{3}{b}\sin(b\ln a)\right]},$$

where H_0 is the Hubble constant. The distance modulus is

$$\mu(z) = m - M = 5\log\frac{d_\mathrm{L}}{10\mathrm{pc}} = 42.39 + 5\log\frac{1+z}{h}\mathcal{F}(z), \tag{4}$$

with $h = H_0/100\,\mathrm{km\ s^{-1}\ Mpc^{-1}}$, where m and M are the apparent and absolute magnitudes, respectively.

2.2 The BAO Data

Since the acoustic oscillations in the relativistic plasma of the early universe will also be imprinted onto the late-time power spectrum of the non-relativistic matter (Eisenstein & Hu 1998), the acoustic signatures in large-scale clusters of galaxies yield additional tests for cosmology (Spergel et al. 2003). Eisenstein et al. (2005) choose a spectroscopic sample of 46 748 luminous red galaxies from SDSS and successfully found the peaks. These galaxies cover 3816 square degrees and have been observed at redshifts up to $z = 0.47$. The peaks are described by the model-independent $\mathcal{A}$-parameter. The $\mathcal{A}$-parameter is independent of the Hubble constant H_0,

$$\mathcal{A} = \frac{\sqrt{\Omega_\mathrm{m}}}{z_1}\left[\frac{z_1}{E(z_1)}\mathcal{F}^2(z_1)\right]^{1/3}, \tag{5}$$

where $z_1 = 0.35$ is the redshift at which the acoustic scale has been measured. Eisenstein et al. (2005) suggested that the measured value of the $\mathcal{A}$-parameter is $\mathcal{A} = 0.469 \pm 0.017$.

2.3 CMB Data

The expansion of the Universe has transformed the black body radiation, which is left over from the Big Bang, into the nearly isotropic 2.73 K CMB (Bernardis et al. 2000). The whole shift of the CMB angular power spectrum is determined by the CMB shift parameter $\mathcal{R}$. The shift parameter, perhaps the most model-independent parameter, is also independent of H_0. It can be derived from CMB data (Bond et al. 1997; Odman et al. 2003),

$$\mathcal{R} = \sqrt{\Omega_\mathrm{m}}\mathcal{F}(z_\mathrm{r}), \tag{6}$$

where $z_\mathrm{r} = 1089$ is the redshift of recombination. Using the Markov Chain Monte Carlo (MCMC) method from the analysis of the three-year results of WMAP (Spergel et al. 2007), Wang & Mukherjee (2006) compute the CMB shift parameter to get $\mathcal{R} = 1.70 \pm 0.03$ and demonstrate that its measured value is mostly independent of assumptions about dark energy.

2.4 $H(z)$ Data from Relative Galaxy Ages

The Hubble parameter $H(z)$ data can be derived from the derivative of redshift z with respect to the cosmic time t, i.e. $\mathrm{d}z/\mathrm{d}t$ (Jimenez & Loeb 2002),

$$H(z) = -\frac{1}{1+z}\frac{\mathrm{d}z}{\mathrm{d}t}. \tag{7}$$

Therefore, an application of the differential age method to old elliptical galaxies in the local universe can determine the value of the current Hubble constant. This is a direct measurement for $H(z)$

through a determination of $\mathrm{d}z/\mathrm{d}t$. Jimenez et al. (2003) have applied the method to a $z \leq 0.2$ sample. Paying careful attention to uncertainties in the distance, systematics, and model uncertainties, they have selected Monte-Carlo techniques to demonstrate its feasibility by evaluating the errors. They also use many other different methods and yield consistent values for the Hubble constant. Hence, the $H(z)$ data are reliable. With the availability of new galaxy surveys, it has become possible to determine $H(z)$ at $z > 0$. By using the differential ages of passively evolving galaxies determined from the Gemini Deep Deep Survey (GDDS) (Abraham et al. 2004) and archival data (Treu et al. 2001; Treu et al. 2002; Nolan et al. 2003a,b), Simon et al. (2005) derived a set of $H(z)$ data, which is listed in Table 1 (see also Samushia & Ratra 2006; Jimenez et al. 2003). The details of the estimation method can be found in the work (Simon et al. 2005). As z has a relatively wide range, $0.1 < z < 1.8$, these data are expected to provide a full-scale description of the dynamical evolution of our universe. The application of the $H(z)$ data to cosmology can be referred to in the works Simon et al. (2005); Yi & Zhang (2007); Samushia & Ratra (2006); Wei & Zhang (2007a); Lin et al. (2009); Gong et al. (2008) and so on.

Table 1 $H(z)$ Data (in units of km s^{-1} Mpc^{-1})

z (redshift)	0.09	0.17	0.27	0.40	0.88	1.30	1.43	1.53	1.75
$H(z)$	69	83	70	87	117	168	177	140	202
1σ error	12.0	8.3	14.0	17.4	23.4	13.4	14.2	14.0	40.4

Simon et al. (2005); see Samushia & Ratra (2006) and Jimenez et al. (2003) also.

3 CONSTRAINTS ON THE UNDULANT UNIVERSE

Considering that the contents of the universe are mainly dark matter and dark energy, we just show $b - \Omega_{\rm m0}$ plane contour maps, where b traces dark energy, and $\Omega_{\rm m0}$ traces dark matter respectively. We estimate the best fit to the set of parameters by using individual χ^2 statistics, with

$$\chi^2_{|\rm data} = \sum_{i=1}^{N} \frac{[d^i_{\rm t}(z) - d^i_{\rm o}(z)]^2}{\sigma_i^2}, \tag{8}$$

where N is the number of data points in each set, $d^i_{\rm t}(z)$ is the value at z_i given by the above theoretical analysis, $d^i_{\rm o}(z)$ is an individual observational value in each data set at z_i, and σ_i is the error due to uncertainties. In order to strengthen the constraints, we use an MCMC technique to modulate the process (Gong et al. 2007). Our results can be seen in Figures 1, 2, 3 and 4.

It is worth noting that the value of h may strongly affect the constraint process, because the probability distribution function (PDF) of h for each data set is different. We can see the PDF for $H(z)$ and SNe Ia data in Figure 5. For $H(z)$ data, we find the PDF of h covers a large range, while it is small for SNe Ia data. Because the distribution of h constrained by SNe Ia is very narrow, if we fix h far from the best-fit, then the constraints will be totally wrong. For example, we test the effect of fixing a "wrong" h by using SNe Ia+BAO+CMB. As can be seen in Figure 6, with a "wrong" h prior, the constraints in the left panel are very different from those in the right panel. This is because if we assume a "wrong" prior for h, the χ^2 would become very large ($\chi^2 \sim 426$ for $h = 0.65$ while $\chi^2 \sim 312$ for $h = 0.7$), and then we will get a false minimum χ^2 that leads to a wrong result. However, if we marginalize the likelihood functions over h by integrating the probability density $P \propto e^{-\chi^2/2}$, we can remove the effect of the distribution of h, and illustrate the reliable distribution of the other parameters. Therefore, we marginalize the likelihood functions over h to obtain the best fitting results. Then we get the confidence regions and the $b - \Omega_{\rm m0}$ plane.

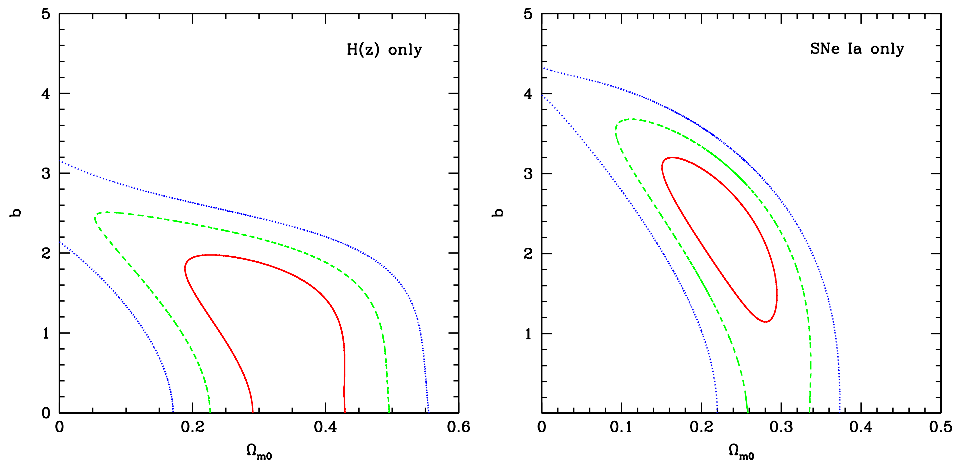

Fig. 1 Contour maps of $b - \Omega_{\rm m0}$ for different data sets. The left panel is $H(z)$ only, and the right panel is SNe Ia only. Confidence regions are at 68.3%, 95.4% and 99.7% levels from inner to outer respectively, for a flat Undulant Universe without a prior of h.

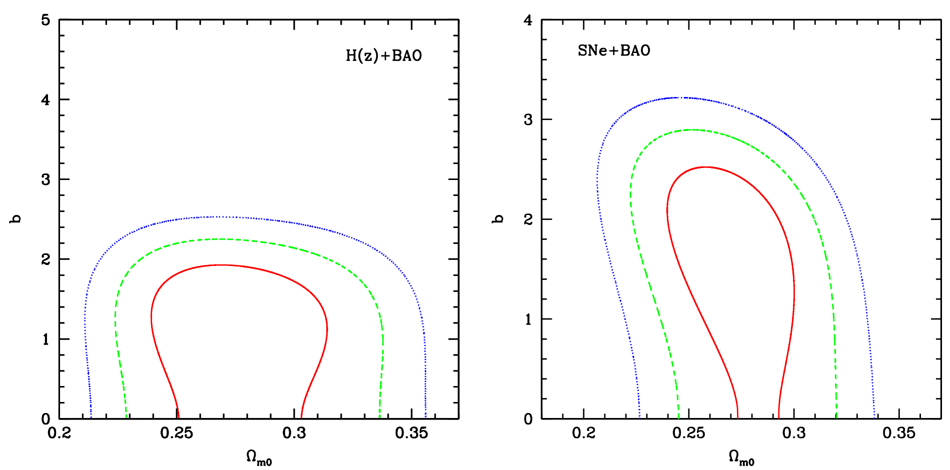

Fig. 2 Contour maps of $b - \Omega_{\rm m0}$ for different data sets. The left panel is $H(z)$+BAO, and the right panel is SNe Ia+BAO. Confidence regions are at 68.3%, 95.4% and 99.7% levels from inner to outer respectively, for a flat Undulant Universe without a prior of h.

As is seen from Equation (1), $\omega(a)$ is an even function. Correspondingly, the values of b along the axis of $\Omega_{\rm m0}$ have a symmetrical distribution. Thus, the constraints on b just in the range from 0 to $+\infty$ are enough to demonstrate the comparison. Figure 1 shows the confidence regions independently determined by the $H(z)$ and SNe Ia data respectively. We find that the constraints on $\Omega_{\rm m0}$ from the $H(z)$ data are weaker than those from the SNe Ia data. Although we just have 9 data points in $H(z)$ data set and 307 data points in the SNe Ia data set, there is still some consistency between them in terms of the constraints. The joint constraints are shown in Figures 2, 3 and 4. We find that

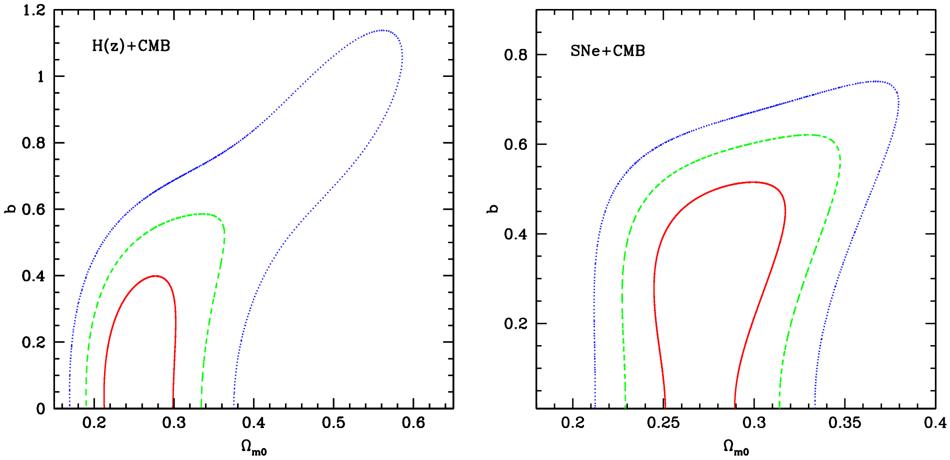

Fig. 3 Contour maps of $b - \Omega_{\rm m0}$ for different data sets. The left panel is $H(z)$+CMB, and the right panel is SNe Ia+CMB. Confidence regions are at 68.3%, 95.4% and 99.7% levels from inner to outer respectively, for a flat Undulant Universe without a prior of h.

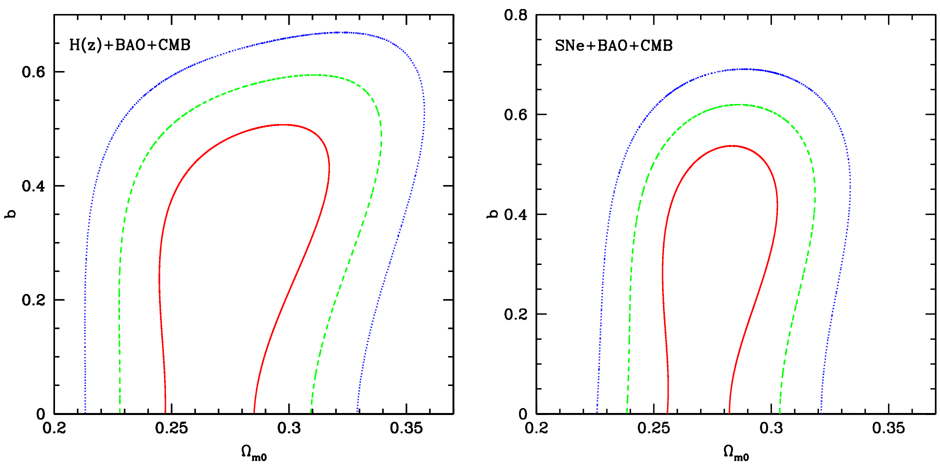

Fig. 4 Contour maps of $b - \Omega_{\rm m0}$ for different data sets. The left panel is $H(z)$+BAO+CMB, and the right panel is SNe Ia+BAO+CMB. Confidence regions are at 68.3%, 95.4% and 99.7% levels from inner to outer respectively, for a flat Undulant Universe without a prior of h.

the constraints are weak if we independently use the $H(z)$ or SNe Ia data, however, after inclusion of the other observational data (the BAO or CMB data), the constraints are remarkably improved. In particular, the CMB data more remarkably improve the constraints. For breaking the degeneracy, the BAO and CMB data play very important roles in the constraint results compared with the $H(z)$ and SNe Ia data sets alone. In the left contour map of Figure 1, and the two contour maps of Figures 2, 3 and 4, all contours at the 1σ confidence for b are open-ended. It shows that b assumes a possible value around 0. We have not demonstrated the details of the constraints, because the MCMC

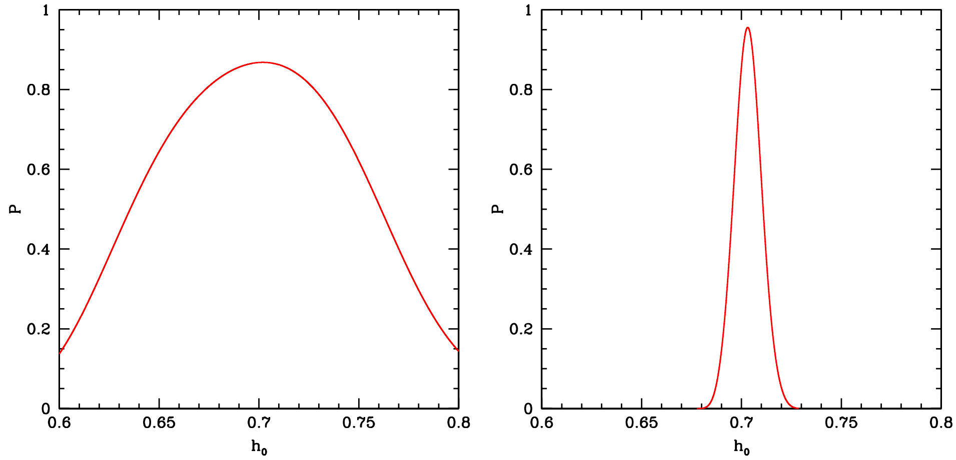

Fig. 5 Probability distribution function of h for $H(z)$ and SNe Ia data, respectively, for a flat Undulant Universe.

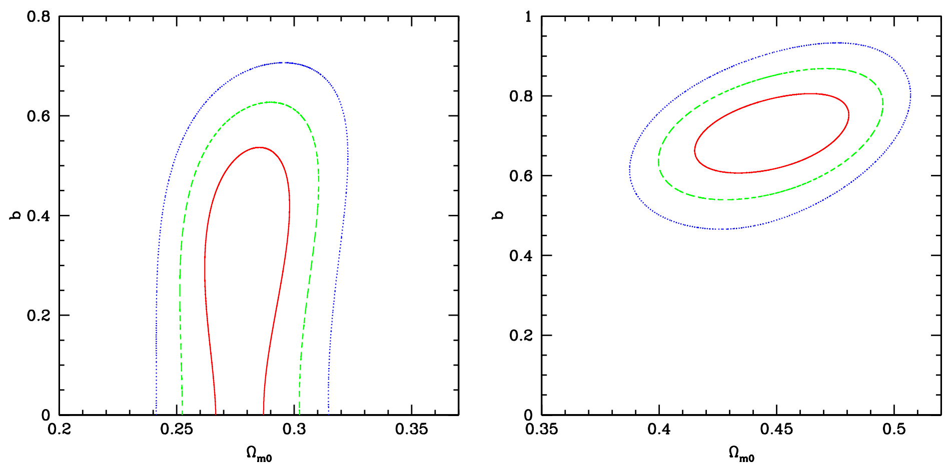

Fig. 6 Contour maps of $b - \Omega_{\rm m0}$ for SNe Ia+BAO+CMB with a "wrong" h prior. h is 0.7 for the left panel, and 0.65 for the right panel. Confidence regions are at 68.3%, 95.4% and 99.7% levels from inner to outer respectively, for a flat Undulant Universe without a prior of h.

technique cannot reliably determine exact values. These contours correspond to $1\sigma, 2\sigma$, and 3σ confidence from inside to outside. Table 2 summarizes 68.3% confidence intervals. From the table, we find that the constraints on $\Omega_{\rm m0}$ from $H(z)$+BAO are looser than those from SNe Ia+BAO, and there is little difference between them. However, the constraints on b from SNe Ia+BAO are looser than those from $H(z)$+BAO. Similar conclusions can be derived from comparing $H(z)$+CMB with SNe Ia+CMB, and $H(z)$+BAO+CMB with SNe Ia+BAO+CMB. The results of $\Omega_{\rm m0}$ in the Undulant Universe are consistent with the recent reported results from the WMAP 5-year data (Kowalski et al. 2008). The distribution of b is close to 0, i.e. the Undulant Universe approaches the ΛCDM model. Comparing Figures 4 and 6, we find that the result of the right panel in Figure 6 with $h = 0.7$ is similar to that of the right panel in Figure 4 when marginalizing h, but has a smaller range for $\Omega_{\rm m0}$.

Table 2 68.3% Confidence Intervals for Each Observational Data Set

Data	$H(z)$	SNe	$H(z)$+BAO	SNe+BAO
$\Omega_{\rm m0}$	$[0.158, 0.43]$	$[0.150, 0.299]$	$[0.239, 0.315]$	$[0.239, 0.305]$
b	$[0, 2.0]$	$[1.13, 3.21]$	$[0, 1.95]$	$[0, 2.47]$
Data	$H(z)$+CMB	SNe+CMB	$H(z)$+BAO+CMB	SNe+BAO+CMB
$\Omega_{\rm m0}$	$[0.21, 0.30]$	$[0.244, 0.318]$	$[0.244, 0.318]$	$[0.253, 0.304]$
b	$[0, 0.40]$	$[0, 0.53]$	$[0, 0.51]$	$[0, 0.58]$

On the other hand, from the result of the left panel in Figure 6 with $h = 0.65$, we find that the range of b shrinks to $0.6 \sim 0.8$ at the 68.3% confidence level and the best-fit value of $\Omega_{\rm m0}$ moves to ~ 0.45, which give the wrong result.

4 CONCLUSIONS AND DISCUSSION

So far, we have presented some constraints on cosmological parameters by using the $H(z)$, SNe Ia, BAO and CMB data in the flat Undulant Universe, and we have marginalized the parameter h to get the best fitting results. If we fix a "wrong" prior for h, any model we use cannot fit the observed data, which leads to a poor χ^2. We show confidence regions in the $b - \Omega_{\rm m0}$ plane. The undulant model can trace the distribution of dark energy in the undulant case. Therefore, our conclusions are more general. As discussed above, we have carefully showed the comparisons between different data sets. Comparing with the independent results of the $H(z)$ and SNe Ia data, the BAO and CMB data play very important roles in breaking the degeneracy. The constraints on $\Omega_{\rm m0}$ from the $H(z)$ data are looser than those from the SNe Ia data, but there is little difference between them. For the combined data sets, the constraints are remarkably improved. The CMB data improve the constraints more remarkably than the BAO data. In the joint constraints, the results from the $H(z)$ data sets ($H(z)$+BAO, $H(z)$+CMB and $H(z)$+BAO+CMB) are almost consistent with those from the SNe Ia data sets (SNe Ia+BAO, SNe Ia+CMB and SNe Ia+BAO+CMB). We find that all the constraints on b are around 0, but the $H(z)$ data sets constrain b more tightly. In particular, the Undulant Universe approaches the ΛCDM model. However, regarding $\Omega_{\rm m0}$, the constraints on the $H(z)$ data sets are weaker than those of the SNe Ia data sets. This is probably because the amount of data is not sufficient and the corresponding errors are very large (Samushia & Ratra 2006). Although there are only nine $H(z)$ data points in our discussion, we still obtain good tight constraints. We speculate that the constraints of the $H(z)$ data sets will be tighter if we get more $H(z)$ data. Therefore, the surplus of $H(z)$ data has an advantage over the SNe Ia data in the constraint. Fortunately, a large amount of $H(z)$ data, including data from the AGN and Galaxy Evolution Survey (AGES) and the Atacama Cosmology Telescope (ACT), are expected to be available in the next few years (Samushia & Ratra 2006). Provided a statistical sample of many hundreds of galaxies, we could determine the value of $H(z)$ data to a percent accuracy. Paying attention to the assumption that SNe Ia act as a "standard candle," it might bias the luminosity distance $d_{\rm L}$ of SNe Ia sample. In addition, there exists an integration of the inverse of $H(z)$ in $d_{\rm L}$, and some uncertainties in the process of minimizing χ^2 statistics might also arise from this integration. On the contrary, $H(z)$ data do not suffer from this uncertainty resulting from integration. Therefore, the $H(z)$ data should constrain parameters more strongly than the SNe Ia data. We also notice that the redshift range of $H(z)$ is from 0.09 to 1.75 and the redshift range of SNe Ia is from about 0.01 to 1.75. Thus, $H(z)$ and SNe Ia are roughly distributed over the same range of redshift values. Therefore, the $H(z)$ data seem to provide us with an independent, very simple, and very powerful probe of fundamental cosmological parameters. With a large amount of the $H(z)$ data in the future, we can probably constrain cosmological parameters by using the $H(z)$ data instead of the SNe Ia data.

Acknowledgements We are very grateful to the anonymous referee for many valuable comments that greatly improved the paper. Tian Lan would like to thank Hui Lin for her valuable discussions, and L. Shao for his help in English. Our MCMC chain computation was performed at the Supercomputing Center of the Chinese Academy of Sciences and the Shanghai Supercomputing Center. This work was supported by the National Natural Science Foundation of China (Grant No. 10473002), the Ministry of Science and Technology National Basic Science program (project 973, Grant No. 2009CB24901), the Fundamental Research Funds for the Central Universities.

References

Abraham, R. G., et al. 2004, AJ, 127, 2455
Alcaniz, J. S., Jain, D., & Dev, A. 2003, Phys. Rev. D, 67, 043514
Barenboim, G., Requejo, O. M., & Quigg, C. 2005, Phys. Rev. D, 71, 063533
Bennett, C. L., et al. 2003, ApJS, 148, 1
Bludman, S. A. 2000, Nucl. Phys. A, 663, 865
Bond, J. R., Efstathiou, G., & Tegmark, M. 1997, MNRAS, 291, L33
Caldwell, R. R., Dave, R., & Steinhardt, P. J. 1998, Phys. Rev. Lett., 80, 1582
Dantas, M. A., Alcaniz, J. S., Jain, D., & Dev, A. 2007, A&A, 467, 421
de Bernardis, P., et al. 2000, Nature, 404, 955
Deffayet, C., Dvali, G., & Gabadagze, G. 2002, Phys. Rev. D, 65, 044023
Efstathiou, G. 1999, MNRAS, 310, 842
Eisenstein, D. J., et al. 2005, ApJ, 633, 560
Eisenstein, D. J., & Hu, W. 1998, ApJ, 496, 605
Garriga, J., Livio, M., & Vilenkin, A. 2000, Phys. Rev. D, 61, 023503
Garriga, J., & Vilenkin, A. 2001, Phys. Rev. D, 64, 023517
Gong, Y., Zhang, T.-J., Lan, T., & Chen, X.-L. 2008, arXiv:0810.3572
Gong, Y., & Chen, X. 2007, Phys. Rev. D, 76, 123007
Jimenez, R., & Loeb, A. 2002, ApJ, 573, 37
Jimenez, R., Verde, L., Treu, T., & Stern, D. 2003, ApJ, 593, 622
Ke, K., & Li, M. 2005, Phys. Lett. B, 606, 173
Kowalski, M., et al. 2008, ApJ, 686, 749
Li, H., Su, M., Fan, Z., Dai, Z., & Zhang, X. 2008, Phys. Lett. B, 658, 95
Lin, H., et al. 2009, Modern Physics Letters A, 24, 1699 (arXiv:0804.3135)
Lineweaver C. H. 1998, ApJ, 505, L69
Maartens, R., et al. 2006, Phys. Rev. D. 74, 023004
Nesseris, S., & Perivolaropoulos, L. 2004, Phys. Rev. D, 70, 043531
Nolan, L. A., Dunlop, J. S., Jimenez, R., & Heavens, A. F. 2003, MNRAS, 341, 464
Nolan, P. L., Tompkins, W. F., Grenier, I. A., & Michelson, P. F. 2003, ApJ, 597, 615
Ödman, C. J., Melchiorri, A., Hobson, M. P., & Lasenby, A. N. 2003, Phys. Rev. D, 67, 083511
Peebles, P. J., & Ratra, B. 2003, Reviews of Modern Physics, 75, 559
Perlmutter, S., et al. 1999, ApJ, 517, 565
Riess, A. G., et al. 1998, AJ, 116, 1009
Samushia, L., & Ratra, B. 2006, ApJ, 650, L5
Simon, J., Verde, L., & Jimenez, R. 2005, Phys. Rev. D, 71, 123001
Spergel, D. N., et al. 2007, ApJS, 170, 377
Spergel, D. N., et al. 2003, ApJS, 148, 175
Stewart, E. D. 2000, in Proceedings of the Fourth International Workshop on Particle Physics and the Early Universe (Cosmo-2000), 147

Tegmark, M., et al. 2000, ApJ, 544, 30
Tegmark, M., et al. 2004, ApJ, 606, 702
Tegmark, M., et al. 2004, Phys. Rev. D, 69, 103501
Tegmark, M., & Rees, M. J. 1998, ApJ, 499, 526
Treu, T., Stiavelli, M., Møller, P., Casertano, S., & Bertin, G. 2001, MNRAS, 326, 221
Treu, T., Stiavelli, M., Casertano, S., Møller, P., & Bertin, G. 2002, ApJ, 564, L13
Vilenkin, A. 2001, arXiv:hep-th/0106083
Wang, Y., & Mukherjee, P. 2006, ApJ, 650, 1
Wei, H., & Zhang, S. N. 2007a, Phys. Lett. B, 644, 7
Wei, H., & Zhang, S. N. 2007b, Phys. Rev. D, 76, 063003
Wu, P., & Yu, H. 2007, Phys. Lett. B, 644, 16
Xia, J.-Q., Zhao, G.-B., Feng, B., Li, H., & Zhang, X. 2006, Phys. Rev. D, 73, 063521
Yi, Z.-L., & Zhang, T.-J. 2007, Modern Physics Letters A, 22, 41
Zhan, H., et al. 2005, Bulletin of the American Astronomical Society, 37, 1202
Zhan, H., et al. 2006, Bulletin of the American Astronomical Society, 38, 1019
Zhang, J., Zhang, X., & Liu, H. 2007, European Physical Journal C, 52, 693
Zhang, H., & Zhu, Z.-H. 2008, Journal of Cosmology and Astro-Particle Physics, 3, 7
Zhang, X., & Wu, F.-Q. 2007, Phys. Rev. D, 76, 023502
Zhao, G.-B., Xia, J.-Q., Li, H., Tao, C., Virey, J.-M., Zhu, Z.-H., & Zhang, X. 2007, Phys. Lett. B, 648, 8
Zhu, Z. H. 2004, A&A, 423, 421